



Minerva Access is the Institutional Repository of The University of Melbourne

Author/s:

Filloramo, GV;Saunders, GW

Title:

Application of multigene phylogenetics and site-stripping to resolve intraordinal relationships in the Rhodymeniales (Rhodophyta)

Date:

2016-06-01

Citation:

Filloramo, G. V. & Saunders, G. W. (2016). Application of multigene phylogenetics and site-stripping to resolve intraordinal relationships in the Rhodymeniales (Rhodophyta). *Journal of Phycology*, 52 (3), pp.339-355. <https://doi.org/10.1111/jpy.12418>.

Persistent Link:

<https://hdl.handle.net/11343/291226>

1
2
3
4
5
6
7
8
9
10
11
12
13
14
15
16
17
18
19
20
21
22
23
24
25
26
27

Received Date : 07-Oct-2015
Revised Date : 01-Feb-2016
Accepted Date : 28-Feb-2016
Article type : Regular Article

Application of multigene phylogenetics and site-stripping to resolve intraordinal relationships in the Rhodymeniales (Rhodophyta)¹

Gina V. Filloramo², Gary W. Saunders

*Centre for Environmental and Molecular Algal Research, Department of Biology,
University of New Brunswick, Fredericton E3B 5A3, New Brunswick, Canada*

Editorial Responsibility: H. Verbruggen (Associate Editor)

¹ Received X XXX 2015. Accepted X XXX 201X

This is the author manuscript accepted for publication and has undergone full peer review but has not been through the copyediting, typesetting, pagination and proofreading process, which may lead to differences between this version and the [Version of Record](#). Please cite this article as [doi: 10.1111/jpy.12418-15-207](https://doi.org/10.1111/jpy.12418-15-207)

This article is protected by copyright. All rights reserved

28 ²Author for correspondence: email gina.filloramo@unb.ca

29 **ABSTRACT**

30 Previous molecular assessments of the red algal order Rhodymeniales have confirmed its
31 monophyly and distinguished the six currently recognized families (viz. Champiaceae,
32 Faucheaceae, Fryeellaceae, Hymenocladaceae, Lomentariaceae, and Rhodymeniaceae);
33 however, relationships among most of these families have remained unresolved possibly as
34 a result of substitution saturation at deeper phylogenetic nodes. The objective of the current
35 study was to improve rhodymenialean systematics by increasing taxonomic representation
36 and using a more robust multigene dataset of mitochondrial (COB, COI/COI-5P), nuclear
37 (LSU, EF2) and plastid markers (*psbA*, *rbcl*). Additionally, we aimed to prevent
38 phylogenetic inference problems associated with substitution saturation (particularly at the
39 interfamilial nodes) by removing fast-evolving sites and analyzing a series of progressively
40 more conservative alignments. The Rhodymeniales was resolved as two major lineages: (i)
41 the Fryeellaceae as sister to the Faucheaceae and Lomentariaceae; and (ii) the
42 Rhodymeniaceae allied to the Champiaceae and Hymenocladaceae. Support at the
43 interfamilial nodes was highest when 20% of variable sites were removed. Inclusion of
44 *Binghamiopsis*, *Chamaebotrys* and *Minium*, which were absent in previous phylogenetic
45 investigations, established their phylogenetic affinities while assessment of two genera
46 consistently polyphyletic in phylogenetic analyses, *Erythrymenia* and *Lomentaria*, resulted
47 in the proposition of the novel genera *Perbella* and *Fushitsunagia*. The taxonomic position
48 of *Drouetia* was reinvestigated with re-examination of holotype material of *D. coalescens*
49 to clarify tetrasporangial development in this genus. In addition, we added three novel
50 Australian species to *Drouetia* as a result of ongoing DNA barcoding assessments—*D.*
51 *aggregata* sp. nov., *D. scutellata* sp. nov., and *D. viridescens* sp. nov.

52

53 **Key Index words:** *Drouetia*; *Erythrymenia*; *Fushitsunagia*; *Lomentaria*; **Multigene**
54 **phylogenetics**; *Perbella*; **Rhodymeniales**; **SiteStripper**.

55 Abbreviations: small subunit ribosomal gene (SSU) PartitionFinder (PF)

56

57 **INTRODUCTION**

58 The Rhodymeniales is a well-studied, species-rich florideophycean order of extremely
59 diverse frond morphologies united by a uniform procarpic female reproductive system (i.e.
60 the auxiliary cell is produced prior to fertilization and in close proximity to the
61 carpogonium within a single branch system) and outward carposporophyte development.
62 Published phylogenetic analyses of florideophycean taxa regard the Rhodymeniales as
63 monophyletic and closely related to the Halymeniales and Sebdeniales (e.g. Saunders &
64 Hommersand 2004, Withall & Saunders 2006, Le Gall & Saunders 2007, Verbruggen et al.
65 2010). Historically, subordinal classification of the Rhodymeniales has been complicated
66 by conflicting perspectives regarding the most useful anatomical features for taxonomic
67 distinction. A brief summary of rhodymenialean systematics is provided below; the reader
68 is referred to Saunders et al. (1999) and Le Gall et al. (2008) for a more comprehensive
69 review.

70 When Schmitz (1889) established the Rhodymeniales, he included six families:
71 Bonnemaisoniaceae, Ceramiaceae, Delesseriaceae, Rhodomelaceae, Rhodymeniaceae and
72 Sphaerococcaceae. Soon after, all of those families were removed except for the
73 Rhodymeniaceae (Oltmanns 1904, Sjöstedt 1926). Bliding (1928) subsequently added the
74 Champiaceae, which was differentiated from the Rhodymeniaceae according to thallus
75 construction (hollow thalli with longitudinal filaments bordering the cavity present vs. solid
76 thalli or hollow thalli but lacking longitudinal filaments), tetrasporangial division patterns
77 (tetrahedral vs. cruciate), number of cells in the carpogonial branch (four vs. three) and the
78 degree to which cells differentiated into carposporangia (only the terminal cells vs. most of
79 the gonimoblast). Kylin (1931) maintained Bliding's two families and further defined them
80 by assigning subfamilies to each. Sparling (1957) rejected Kylin's subclassifications and
81 emphasized the presence (Champiaceae) or absence (Rhodymeniaceae) of longitudinal
82 filaments bordering the hollow parts of thalli for family-level distinction. Later, Lee (1978)
83 used a combination of vegetative (thallus septation) and reproductive criteria (number of
84 cells in the carpogonial branch and the position of the tetrasporangia) to define the
85 Champiaceae, Rhodymeniaceae, and a third family, Lomentariaceae. Lee's three-family
86 classification system was widely accepted; however, some rhodymenialean genera featured
87 diagnostic characters of more than one family and, therefore, could not be classified

88 confidently (e.g., *Dictyothamnion*, *Ceratodictyon*, *Gelidiopsis*, *Hymenocladia*,
89 *Hymenocladopsis* and *Semnocarpa*, see Saunders et al. 1999).

90 The application of molecular techniques to systematic studies of the red algae has
91 enabled a more objective means of assessing evolutionary relationships within the
92 Rhodymeniales. Although rhodymenialean taxa were represented in some of the earliest red
93 algal molecular phylogenetic investigations (e.g., Freshwater et al. 1994, Ragan et al. 1994,
94 Saunders & Kraft 1994, Saunders & Kraft 1996), these studies only included enough taxa
95 to establish the order as monophyletic and allied to the Halymeniales. Subordinal
96 relationships remained largely unresolved until Saunders et al. (1999), using the nuclear
97 small subunit ribosomal gene (SSU), embarked on the first extensive molecular systematic
98 study specific to the Rhodymeniales. That study included 56% of the recognized genera
99 (Saunders et al. 1999). Challenging Lee's three-family system, Saunders et al. (1999)
100 resolved the Rhodymeniales as six monophyletic assemblages distributed in two major
101 lineages – the first included only a reduced Rhodymeniaceae while the second consisted of
102 the Champiaceae, Lomentariaceae, their newly established Faucheaceae, and two
103 unassigned lineages. In light of their results, Saunders et al. (1999) emphasized
104 reproductive features, including the number of cells in the carpogonial branch,
105 tetrasporangial cleavage patterns and tetrasporangial position for family-level classification.
106 Although that study was significant for providing a more natural system of classification
107 for the Rhodymeniales, it was limited by its low representation of rhodymenialean taxa
108 (both the absence of entire genera and many generitype species) and lack of resolution
109 among interfamilial nodes (Saunders et al. 1999). Poor resolution was partially due to gene
110 choice as SSU displayed highly variable rates in some families, which increased the
111 potential for long-branch attraction artefacts (Saunders et al. 1999). In a subsequent study
112 Le Gall et al. (2008) sought to circumvent potential long-branch attraction artefacts by
113 increasing taxonomic representation (by ~13%) and basing phylogenetic inference on two
114 nuclear genes: elongation factor 2 (EF2) and the large-subunit nuclear ribosomal DNA
115 (LSU). Le Gall et al. (2008) again resolved six fully supported family-level lineages.
116 Although their newly described Fryeellaceae was strongly allied to the sister families

117 Faucheaceae and Lomentariaceae, the relationships among the remaining families remained
118 inconclusive (Le Gall et al. 2008).

119 The inability of the previous molecular phylogenetic analyses to generate
120 meaningful interfamilial support was due at least in part to the general difficulty of
121 obtaining strong phylogenetic signal for lineages that have diverged deeper in evolutionary
122 time (Verbruggen et al. 2009, Pisani et al. 2012, Zeng et al. 2014). Although a common
123 approach for improving phylogenetic inference is to use larger datasets (Holton & Pisani
124 2010), increasing the number of taxa and genes does not guarantee that signal at deeper
125 epochs of interest will be enhanced and this approach may actually increase the potential
126 for systematic errors (Jeffroy et al. 2006, Sperling et al. 2009, Pick et al. 2010). One of the
127 major challenges for resolving deep evolutionary relationships is overcoming issues
128 associated with substitution saturation at quickly evolving sites (Cocquyt et al. 2010).
129 Typically deep phylogenetic nodes are recorded in the historical signal of the more slowly
130 evolving positions in an alignment; however, the stochastic noise introduced by quickly
131 evolving sites can overwhelm this signal, which can lead to incorrect or poorly supported
132 deep phylogenetic nodes (Ho & Jermiin 2004, Kostka et al. 2008). Fast site removal (site-
133 stripping) is one technique that has been applied to reduce issues associated with systematic
134 errors and substitution saturation to facilitate resolution of deeper relationships (Ruiz-Trillo
135 et al. 1999, Morgan-Richards et al. 2008, Cocquyt et al. 2010). By removing quickly
136 evolving sites, the signal to noise ratio is increased so that the signal of the historically
137 informative more slowly evolving sites is maximized (Brinkmann & Philippe 1999,
138 Waddell et al. 1999, Delsuc et al. 2005, Rodríguez-Ezpeleta et al. 2007, Kostka et al. 2008).
139 The command line program SiteStripper (Verbruggen 2012) was originally designed to
140 better resolve deep nodes within the Ulvophyceae (Chlorophyta). SiteStripper
141 systematically removes variable sites from an alignment, 5% each time, to create a series of
142 progressively more conservative sub-alignments that can be analyzed by phylogenetic
143 inference techniques (Cocquyt et al. 2010). One of those sub-alignments should have
144 enough of the quickly evolving sites removed while retaining sufficient signal to elucidate
145 deeper relationships (Cocquyt et al. 2010).

146 The goals of the present study were: 1) to reassess and improve rhodymenialean
147 systematics by expanding taxonomic representation (in conjunction with the Red Algal
148 Tree of Life project, <http://dmlab.rutgers.edu/redtol/home.php>) and generating a more robust
149 multigene dataset of mitochondrial (COB & COI/COI-5P), nuclear (EF2 & LSU) and
150 plastid (*psbA* & *rbcL*) markers; 2) to minimize phylogenetic inference problems associated
151 with substitution saturation and improve resolution at interfamilial nodes by assessing this
152 dataset with a fast-site removal reconstruction technique (SiteStripper); 3) to revisit the
153 classification system proposed by Le Gall et al. (2008) based on our generated topology; 4)
154 to establish the phylogenetic affinities of some genera (*Binghamiopsis*, *Chamaebotrys*, and
155 *Minium*) absent from previous large-scale phylogenetic studies; 5) to assess genera
156 consistently polyphyletic in published molecular analyses (notably *Erythrymenia* and
157 *Lomentaria*); 6) to reinvestigate the taxonomic position of the problematic genus *Drouetia*;
158 and, 7) to characterize novel taxa included in our analyses.

159

160 MATERIALS AND METHODS

161 *Phylogenetic Analyses.* Specimens used in phylogenetic analyses (Table S1) were pressed
162 on herbarium paper or dried in silica to serve as vouchers with subsamples preserved in
163 silica for molecular analyses. Genomic DNA was extracted following Saunders & McDevit
164 (2012) with amplification of the following markers following Saunders & Moore (2013):
165 the mitochondrial cytochrome b gene (COB); the mitochondrial cytochrome c oxidase
166 subunit 1 extended fragment or barcode region (COI and COI-5P, respectively); the nuclear
167 elongation factor 2 gene (EF2); the nuclear large-subunit ribosomal RNA gene (LSU); the
168 plastid photosystem II thylakoid membrane protein D1 (*psbA*); and the plastid ribulose-1,
169 5-biphosphate carboxylase large subunit gene (*rbcL*) (Table S1). Amplicons were
170 sequenced by the Génome Québec Innovation Centre and raw data were edited in
171 Sequencher™ 5.0 (Gene Codes Corporation, Ann Arbor, MI, USA) and aligned in
172 Geneious R7 version 7.1.7 (<http://www.geneious.com>, Kearse et al. 2012) with additional
173 sequences acquired from GenBank (Table S1 in the Supporting Information).

174 Six single-gene alignments were produced [COB (49% of ingroup taxa, 942 bp);
175 COI/COI-5P (90% of ingroup taxa, 1232 bp); EF2 (72% of ingroup taxa, 1641 bp); LSU

176 (100% of ingroup taxa, 2588 of 2841bp included in analyses.); *psbA* (62% of ingroup taxa,
177 953 bp) and *rbcL* (89% of ingroup taxa, 1358 bp); (Table S1)] and analyzed independently
178 using Bayesian inference and Maximum likelihood under the GTR+I+G model with
179 partitioning by codon for protein-coding genes. Bayesian analyses were completed using
180 MrBayes v.3.2.1 (Ronquist & Huelsenbeck 2003) in Geneious R7 version 7.1.7 with
181 parameter settings (Tratio, Revmat, Statefreq, Pinvar, Shape, Switchrates) unlinked, rate
182 differentiation across the partitions enabled and branch lengths unconstrained with the
183 branch length priors set to exponential (default exponential prior setting: 10.0). Analyses
184 were run in parallel for 1,000,000 generations with sampling performed every 100
185 generations. The burn-in was determined when both analyses converged into the stationary
186 phase. Maximum likelihood analyses were performed using RAxML in Geneious R7
187 version 7.1.7 with a non-parametric bootstrap of 1,000 replicates.

188 All genes resolved congruent phylogenetic relationships and were combined to
189 generate a multigene alignment (8,714 bp, 78% complete by site) for further phylogenetic
190 analyses. Percent completeness for each taxon included in this study was recorded in Table
191 S1. The multigene alignment was analyzed by Bayesian inference and Maximum likelihood
192 under the GTR+I+G model with parameters settings as specified above with the exception
193 of running Bayesian analyses for 3,500,000 generations with sampling performed every
194 3,500 generations. The impact of partitioning was evaluated by completing analyses first by
195 partitioning data by gene and codon (noPF) and then according to the evolutionary models
196 and partitioning schemes determined by implementing PartitionFinder (PF) (Lanfear et al.
197 2012) under the BIC model selection criteria with linked branch length estimation. To
198 assess the impact of missing data, Bayesian and Maximum likelihood analyses were
199 repeated after first removing taxa less than 50% (n= 8) complete by site and then removing
200 taxa less than 70% (n= 25) complete by site.

201
202 *Site-Stripping*. To assess the impact of substitution saturation on phylogenetic inference,
203 site-specific rates were calculated for the multigene alignment using the program HyPhy
204 (Pond et al. 2005) under the JC69 model with a Bayes phylogram as a guide tree.
205 SiteStripper (Verbruggen 2012) was used to order sites by rate and then remove quickly

206 evolving sites, 5% at a time, to generate a series of progressively more conservative sub-
207 alignments that were analyzed using RAxML version 7.3.5 (Stamatakis 2012) with a
208 command line script available through SiteStripper. Analyses were partitioned by gene and
209 then codon (noPF) under a GTR+I+G model and with the partitioning schemes and models
210 of evolution as determined by PartitionFinder (PF). Branch support was estimated by 1,000
211 non-parametric bootstrap replicates.

212 To determine if site-stripping biases downstream analyses towards the phylogeny
213 used as a guide tree, we recalculated site rates using an alternative starting tree topology
214 (Supplementary Fig. S1) that was generated using a neighbor-joining analysis under the
215 HKY genetic distance model in Geneious R7. The resulting site rates were used by
216 SiteStripper to generate a series of subalignments, which were analyzed by RAxML. To
217 assess the neighbor-joining tree against the original starting tree (Bayesian Inference tree
218 with partitioning by gene and codon), the Shimodaira-Hasegawa test (“-f h” option) was
219 implemented using RAxML.

220

221 *Barcode analyses*

222 A total of 16 collections field identified to the genus *Drouetia* were collected from the
223 subtidal in Coffs Harbour, New South Wales, Australia (Table 1) and dried in silica gel
224 with voucher preservation, DNA extraction, and COI-5P amplification, sequencing, editing
225 and aligning as outlined above. The DNA barcode alignment (664 bp) was analyzed in
226 BOLD to determine intraspecific variation and nearest neighbour distances.

227

228 *Morphological analyses.* Vegetative and reproductive features were analyzed by
229 rehydrating algal tissue in 5% formalin and seawater and preparing sections using a
230 freezing microtome (Leica CM1850, Leica Microsystems, Wetzlar, Germany). Sections
231 were stained with 1% analine blue solution in 6% 5N hydrochloric acid, rinsed with
232 distilled water and permanently mounted in 50% corn syrup with 4% formalin. Photographs
233 were taken using a Leica digital camera (DFC480) mounted to a Leica microscope
234 (CTR5000) and plates were made using Adobe Photoshop Elements 11 (2012).

235

RESULTS

236

237

238

239

240

241

242

243

244

245

246

247

248

249

250

251

252

253

254

255

256

257

258

259

260

261

262

263

264

265

To resolve subordinal relationships among the Rhodymeniales, a six gene concatenated alignment (80 species representing 42 genera) was assessed using Bayesian analysis and Maximum likelihood (ML). Analyses were completed using the model GTR+I+G with partitioning by gene and codon. Then, analyses were performed again according to the model (GTR+I+G) and partitioning scheme (LSU) (COB1) (COB2, *psbA1*) (COB3, COI3) (COI1, *rbcL1*) (COI2, *psbA2*, *rbcL2*) (EF21) (EF22) (EF23) (*psbA3*) (*rbcL3*) as determined by PartitionFinder. The phylogram inferred by ML analysis with partitioning by gene and then codon is presented (Fig. 1) with bootstrap support values shown for subfamilial branches. Familial and interfamilial branch support are presented separately (Table 2). The topology in Fig. 1 was resolved for all analyses of the full alignment except Bayesian inference with partitioning by gene and then codon, which failed to resolve branch C (lacked support in all full alignment analyses) (Table 2). Posterior probabilities and bootstrap support values were essentially not changed whether the alignment was fully partitioned or used the scheme selected by PartitionFinder. For both Bayesian and ML analyses, tree scores were slightly better when data were partitioned by gene and codon rather than the partitioning schemes as defined by PartitionFinder (Table 2). Exclusion of incomplete taxa (both those < 50% and < 70% complete by site, Table S1) did not change the tree topology (Fig. 1) and had little impact on posterior probabilities and bootstrap support values (data not shown). Maximum likelihood analyses of the progressively more conservative sub-alignments (partitioned by gene and codon only) produced the same tree topology (Fig. 1) as analyses of the full dataset; however, interfamilial branch support increased at three key branches (Table 2, branches B, C & I) with optimal signal gained when 20% of the quickly evolving sites were eliminated (i.e. 80% of the sites were retained). The results of the Shimodaira-Hasegawa test indicated that the neighbor-joining guide tree topology (likelihood -144156.83, Fig. S1) was significantly different ($p < 0.01$) than the Bayes guide tree topology (likelihood -143596.69). Despite the previous, use of the neighbor-joining topology as the guide tree for calculating sites rates did not impact downstream site-stripping analyses as support for interfamilial and familial branches was consistent with SiteStripping analyses that used a Bayes guide tree.

266 All analyses (i.e. full alignment, site-stripped alignments, those for which
267 incomplete taxa were removed) solidly resolved the Rhodymeniales (branch A, Fig. 1,
268 Table 2) as comprised of six monophyletic families distributed in two major lineages. The
269 first lineage (branch B, Fig. 1) was strongly resolved in all analyses and included the
270 Faucheaceae (branch G, Fig. 1), Fryeellaceae (branch D, Fig. 1) and Lomentariaceae
271 (branch F, Fig. 1). The second lineage (branch C, Fig. 1) included the Champiaceae
272 (branch J, Fig. 1), Hymenocladaceae (branch K, Fig. 1) and Rhodymeniaceae (branch H,
273 Fig. 1) and was variably supported in analyses of the full alignment; however, support at
274 branch C increased (up to 75%, Table 2) as quickly evolving sites were removed. Within
275 the first lineage the sister relationship of the Faucheaceae to the Lomentariaceae
276 (interfamilial branch E; Fig. 1) was fully supported across all analyses (Table 2). Within the
277 second lineage, the Champiaceae was moderately resolved (Table 2) as sister to the
278 Hymenocladaceae (interfamilial branch I, Fig. 1). Support at branch I (Fig. 1; Table 2)
279 initially decreased (down to 71%, Table 2) when 5% of the quickly evolving sites were
280 removed (i.e. 95% of the sites were retained) and continued to fluctuate up and down with
281 the generation of each sub-alignment; however, support was highest (81%, Table 2) when
282 20% of the sites were eliminated.

283 Analyses resolved phylogenetic relationships for genera included in a molecular
284 context for the first time. The monospecific genus *Binghamiopsis* was positioned within the
285 Lomentariaceae and strongly associated with *Lomentaria hakodatensis* (Fig. 1). Within the
286 Rhodymeniaceae, *Chamaeobotrys* (represented by the generitype *C. boergesenii* and an
287 unidentified species from Australia) was solidly allied to the sister genera *Halichrysis* and
288 *Halopeltis* (Fig. 1), while collections assigned to the genus *Drouetia* were resolved as a
289 fully supported monophyletic lineage distantly related to a lineage containing species of
290 *Chrysymenia* and *Maripelta* (Fig. 1). The monospecific genus *Minium* was fully resolved
291 within the Fryeellaceae as an unexpectedly close sister to *Fryeella gardneri* (Fig. 1).

292 Inclusion of select generitype species enabled assessment of monophyly for a few
293 genera. Within the Hymenocladaceae, species of *Erythrymenia* failed to form a
294 monophyletic lineage with *Erythrymenia minuta* sister to *Hymenocladia* spp. rather than the
295 type of the genus, *Erythrymenia obovata* (Fig. 1). The genus *Perbella* was established

296 (below) to accommodate *Erythrymenia minuta* and render *Erythrymenia* monophyletic.
297 Within the Lomentariaceae, species of *Lomentaria* were resolved as four independent
298 lineages: (i) the generitype *L. articulata* joined *L. clavellosa* and *L. orcadensis* to form a
299 fully supported monophyletic lineage; (ii) *L. catenata* and *Ceratodictyon* spp. were allied
300 with full support; (iii) *L. divaricata* resolved as sister to *Stirnia*; and (iv) *L. hakodatensis*
301 was fully resolved as sister to *Binghamiopsis* (Fig. 1). The genus *Fushitsuagia* was
302 established to accommodate *L. catenata* while the generic assignments of *L. divaricata* and
303 *L. hakodatensis* could not formally be determined at this time (discussed below).

304 Analyses resolved some additional genera as polyphyletic (Fig 1). Rather than
305 resolving with other species of *Botryocladia*, the species *B. leptopoda* was more closely
306 allied with *Chrysymenia wrightii* (which failed to resolve with other included *Chrysymenia*
307 spp.; Fig. 1). The species *R. delicatula* was resolved as relatively distinct from other species
308 of *Rhodymenia* (including the generitype) and was most closely related to *Cordylecladia*
309 *erecta* (Fig. 1).

310 Sixteen collections from Coffs Harbour, New South Wales, Australia were resolved
311 as three genetic species groups and assigned to the genus *Drouetia* as novel taxa (see
312 below). Maximum COI-5P intraspecific divergence for these species was 0.31% (Table 3).
313 The nearest neighbour to *D. aggregata* was *D. scutellata* (7.19% divergent, Table 3) while
314 the closest species to *D. scutellata* was *D. viridescens* (2.5% divergent, Table 3). The
315 species *D. scutellata* and *D. viridescens* were included in multigene analyses where they
316 were resolved in the Rhodymeniaceae and distantly related to an unidentified species of
317 *Drouetia* from South Africa (Fig. 1).

318

319 *Taxonomic Treatment*

320 ***Drouetia aggregata*** Filloramo & G.W. Saunders, **sp. nov.** (Fig. 2)

321 *Description.* Blades irregular in outline, peltate, typically anastomosing where they overlap
322 (Fig. 2a), stipe 12-15 mm long x 2 mm wide (Fig. 2b); blades ca. 950 µm in transverse
323 section at mid-thallus with 9-13 medullary layers of large axially elongated, non-pigmented
324 cells (250-400 µm long x 80-100 µm wide) with frequent secondary pit connections (Fig.
325 2c) and distinct aggregations of smaller, round cells (50 µm in diameter; Fig. 2d);

326 medullary cells typically reducing in size toward the ~2 inner cortical layers of smaller cells
327 subtending a dorsal cortex of 2-3 layers of densely packed, columnar-shaped, darkly
328 staining cells (~10 µm in diameter) and a single-layered ventral cortex of larger round cells
329 (15-18 µm in diameter; Fig. 2c); dorsal and ventral cuticle, 10 µm and 7.5 µm thick,
330 respectively (Fig. 2c). Reproductive structures not observed.

331 *Holotype*. GWS032793 collected on December 12, 2012 at Mutton Bird Island (South),
332 Coffs Harbour, New South Wales, Australia (-30.30467, 153.14796), by G.W. Saunders
333 and K. Dixon and deposited in the Connell Memorial Herbarium (UNB) of the University
334 of New Brunswick, Fredericton, Canada. Images of holotype Figures 2, a-c.

335 *Holotype COI-5P Barcode*. KU707873.

336 *Isotype*. GWS032792 (deposited in UNB, Table 1).

337 *Etymology*. Named for the aggregates of small cells interspersed throughout the larger cells
338 of the medulla – this feature being pronounced when compared to other species of *Drouetia*.

339 *Geographical Distribution*. Thus far only known from the type location.

340 *Comments*. *Drouetia aggregata* is distinguished from the other species of *Drouetia* in
341 Australia owing to its long stipe, thick thallus in cross section, larger medullary cells, and
342 the aggregation of small round cells interspersed among the other medullary cells.

343

344 ***Drouetia scutellata*** Filloramo & G.W. Saunders, **sp. nov.** (Fig. 3)

345 *Description*. Peltate blades depressed at center and borne on short, narrow stipes 6-10 mm
346 long x 0.5 mm wide (Fig. 3a); blades typically remaining saucer-shaped upon maturity, at
347 times anastomosing at the margins (Fig. 3b); blades ca. 250-375 µm thick in transverse
348 section at mid-thallus with (3-) 4-5 medullary layers of large elongated cells (90-145 µm
349 long x 72-87.5 µm wide) grading to 1-2 inner cortical layers of elongated cells subtending 2
350 dorsal cortical layers of darkly staining cells (12.5 µm in diameter) and 2 ventral layers of
351 slightly larger rounded cells (17.5 µm in diameter; Fig. 3c8). Plants dioecious. Cystocarps
352 clustered centrally on dorsal (upper) blade surface (Fig. 3b), rounded, ostiolate, 800-1000
353 µm in diameter, nutritive tissue present at base (Fig. 3d). Spermatangial sori formed on the
354 dorsal surface with spermatangia cut off from elongated spermatangial mother cells (Fig.
355 3e). Tetrasporophytes not observed.

356 *Holotype*. Female gametophyte GWS032729 collected on December 11, 2012 at Mutton
357 Bird Island (North), Coffs Harbour, New South Wales, Australia (-30.304706, 153.150959),
358 by G.W. Saunders and K. Dixon and deposited in the Connell Memorial Herbarium (UNB)
359 at the University of New Brunswick, Fredericton, Canada. Images of holotype Figure 3, b
360 and d.

361 *Holotype COI-5P Barcode*. KU707880

362 *Isotype*. Male gametophyte GWS032752 (deposited in UNB; Table 1).

363 *Etymology*. Named for the plant's typically saucer-shaped blades.

364 *Representative specimen examined*. GWS032664 (deposited in UNB, see Table 1 for
365 collection details).

366 *Geographical Distribution*. Thus far known only from the type location and nearby South
367 Solitary I., Coffs Harbour, New South Wales, Australia.

368 *Comments*. *Drouetia scutellata* features a thin thallus in cross section with few medullary
369 cell layers rendering it rather distinct when compared to other species of *Drouetia* from
370 Australia. Differences in internal anatomy are especially useful for distinguishing between
371 *D. scutellata* and *D. viridescens*, which also has a single peltate blade with a depressed
372 center and short stipe. Additionally, while some reproductive plants of *D. scutellata* have
373 been encountered as single blades, reproductive plants of *D. viridescens* have only been
374 observed as anastomosed blades (below).

375

376 ***Drouetia viridescens*** Filloramo & G.W. Saunders, **sp. nov.** (Fig. 4)

377 *Description*. Juvenile blades peltate with shallow central depression (Fig. 4a), becoming
378 stellate or lobed with age and typically anastomosing at margins and where blades overlap
379 (Fig. 4b), borne on a short stipes 3-6 mm long x 1 mm wide. Transverse sections at mid-
380 thallus 310-500 μm thick with 9-12 medullary layers of large, axially elongated cells (90-
381 140 μm long x 50-80 (-120) μm wide) decreasing in size to 2 dorsal cortical layers of small,
382 densely packed, darkly staining cells (10-15 μm in diameter) and 1-2 ventral cortical layers
383 of round darkly staining cells (17.5-20 μm in diameter); outgrowths of the ventral cortical
384 cells presumably involved in secondary attachments to substratum and other blades (Fig. 4,
385 c and d); dorsal (~7.5 μm thick) and ventral cuticles (5 μm thick) obvious (Fig. 4c).

386 Tetrasporangial sori confined to the dorsal surface (Fig. 4d), tetrasporangia cruciately
387 divided (30-40 μm long x 15-20 μm wide; Fig. 4e), differentiating from existing cortical
388 cells (Fig. 4, f-g); all outer cortical cells appear capable of differentiating into sporangia but
389 do not convert simultaneously causing undifferentiated cortical cells to become elongated
390 and compressed between developing tetrasporangia giving the appearance of paraphyses
391 (Fig. 4, f-g). Cystocarps and spermatangia not observed.

392 *Holotype*. Tetrasporophyte GWS032612 collected on December 9, 2012 in Split Solitary
393 Island (Northwest) Coffs Harbour, New South Wales, Australia (-30.24210, 153.17921), by
394 G.W. Saunders and K. Dixon and deposited in the Connell Memorial Herbarium (UNB) at
395 the University of New Brunswick, Fredericton, Canada. Images of holotype Figure 4, b, d-
396 g .

397 *Holotype COI-5P Barcode*. KU707855

398 *Isotype*. GWS032624 (Table 1).

399 *Etymology*. The species epithet acknowledges the plant's green iridescent glow underwater
400 observed at the time of collection.

401 *Representative specimens examined*. GWS032599, GWS032600, GWS032642,
402 GWS032643, GWS032665, GWS032672, GWS032682, GWS032740, GWS032790
403 (deposited in UNB, see Table 1 for collection details).

404 *Geographical Distribution*. Thus far known only from the type locality and nearby sites in
405 Coffs Harbour, New South Wales, Australia.

406 *Comments*. This species has the shortest stipe and the center of the blade typically "glows"
407 green when encountered underwater. Although *D. viridescens* has a similar number of
408 medullary cell layers as *D. aggregata*, the former is much thinner in cross section with
409 smaller medullary cells. The upper range of thallus thickness for *D. scutellata* overlaps with
410 the lower range for *D. viridescens*; however, the fewer number of medullary cell layers for
411 *D. scutellata* distinguishes it from the latter.

412

413 ***Generitype observations of Drouetia coalescens*** (Farlow) G. De Toni (Fig. 5)

414 Holotype material of *D. coalescens* was provided on loan from the Farlow Herbarium (FH)
415 (Fig. 5a). Blades were ca. 500 μm thick with 8-11 medullary cell layers of typically axially

416 elongated cells of varying sizes (Fig. 5b). The dorsal blade surface was ca. 3 cortical layers
417 thick while the ventral surface was composed of up to 6 layers of small, round, tightly
418 packed cells subtending a thick cuticle (Fig. 5b). Tetrasporangia were observed as deeply
419 embedded in only the dorsal cortex (Fig. 5, b and c), cruciately divided (52-55 μm long x
420 15-18 μm wide; Fig. 5d) with the tetrasporangial initials arising from the cells of the inner
421 cortex (Fig. 5e). As the tetrasporangia matured, they lengthened and swelled causing
422 neighboring cortical cells to become compressed and elongated between the developing
423 tetrasporangia, taking on the appearance of paraphyses (Figs. 5c-e).

424 *Comments.* The generitype species shares a similar gross morphology with the novel
425 species *D. aggregata* and *D. viridescens* in that all three species feature decumbent, peltate
426 blades, which commonly anastomose at the margins. Compared to *D. aggregata*, the
427 generitype is thinner in cross section and lacks aggregations of small cells within the
428 medulla. The generitype species features longer tetrasporangia compared to those of *D.*
429 *viridescens* and has never been reported to “glow” green underwater as is diagnostic of *D.*
430 *viridescens*. Although the habitat of the type specimen of *D. coalescens* is unknown, Taylor
431 (1945) collected material from the low-intertidal that was observed by Saunders et al. (2006)
432 who recognized it as morphologically consistent with *D. coalescens*. According to the
433 previous, *D. coalescens* is distinct in its intertidal habitat relative to the three Australian
434 *Drouetia* species, which have only been collected subtidally.

435

436 ***Fushitsunagia*** Filloramo & G.W. Saunders, **gen. nov.**

437 *Diagnosis:* Lomentariacean algae with hollow thalli divided by multi-rowed cellular septa.
438 Spermatangial sori are borne on specialized fertile ramuli. The cells of the medulla become
439 elongated and stretched appearing almost filamentous as they form a conspicuous stellate
440 network surrounding the developing tetrasporangia, which, when mature, are tetrahedrally
441 divided.

442 *Etymology:* In recognition of the Japanese name “*Fushitsunagi*” (“fushi”= joint, knot, and
443 node; “tsunagi”= connection) that was assigned to *Lomentaria catenata* by Okamura (Lee
444 1978).

445 *Type and only species: Fushitsunagia catenata* (Harvey) Filloramo & G.W. Saunders,
446 **comb. nov.**
447 *Basionym: Lomentaria catenata* Harvey 1857 (Algae. In: Account of the Botanical
448 specimens. Gray, A., [Eds.] *Narrative of the expedition of an American squadron to the*
449 *China Seas and Japan, performed in the years 1852, 1853 and 1854, under the command of*
450 *Commodore M.C. Perry, United States Navy. Volume II – with illustrations.* Anon. [Eds.].
451 Senate of the Thirty-third Congress, Second Session, Executive Document. House of
452 Representatives, Washington, USA, pp. 331-332).

453

454 **Perbella** Filloramo & G.W. Saunders, **gen. nov.**

455 *Diagnosis:* Hymenocladacean algae with smaller cells intermixed among the larger
456 medullary cells from which they likely develop. Tetrasporangia are decussately divided.

457 *Etymology:* Latin for “very beautiful”, attributed to the breathtaking appearance of the type
458 species when observed underwater or immediately after collection.

459 *Type and only species: Perbella minuta* (Kylin) Filloramo & G.W. Saunders, **comb. nov.**

460 *Basionym: Erythrymenia minuta* Kylin 1931 [Die Florideenordnung Rhodymeniales. *Acta*
461 *Universitatis Lundensis* 27(11):1-48].

462

463 DISCUSSION

464 *Interfamilial relationships*

465 The present study represents the most comprehensive molecular phylogenetic analysis of
466 the Rhodymeniales based on the number of taxa included and markers used. Further, we
467 have applied a technique to remove the most rapidly evolving sites from our multigene
468 alignment to enhance resolution at the interfamilial nodes (Fig. 1). Results were largely
469 congruent with previously published phylogenetic assessments of the order (Saunders et al.
470 1999, Le Gall et al. 2008) in that all of our analyses resolved the Rhodymeniales as
471 comprised of six monophyletic families (Fig. 1); however, those previous studies
472 consistently resolved only an alliance between the Faucheaceae and Lomentariaceae
473 (Saunders et al. 1999, Le Gall et al. 2008) while the current study resolved most
474 interfamilial relationships with solid support (Fig. 1, Table 2). The Faucheaceae and

475 Lomentariaceae were resolved as sister groups and allied to the Fryeellaceae while the
476 Champiaceae and Hymenocladaceae were resolved together and associated with the
477 Rhodymeniaceae (Fig. 1). Site-Stripping had the greatest impact on the short internal
478 branch (branch C, Fig. 1) leading to the Champiaceae, Hymenocladaceae and
479 Rhodymeniaceae. It is possible that this branch represents a lineage that radiated over a
480 short period of evolutionary time. Generally, the limited signal associated with short
481 branches is masked by more recent substitution events, which impacts accurate resolution
482 of evolutionary relationships occurring over those short time intervals (Pisani et al. 2012).
483 Removing the quickly evolving sites (i.e. those prone to substitution saturation) from our
484 original alignment reduced the stochastic noise and uncovered the historical signal. We
485 were able to provide meaningful resolution for previously unresolved relationships within
486 the Rhodymeniales. The interfamilial relationships resolved herein were consistent with the
487 classification system proposed by Le Gall et al. (2008) emphasizing ontogeny of the
488 tetrasporangia.

489

490 *Taxa included in molecular analyses for the first time*

491 Molecular data solidly resolved the monospecific genus *Binghamiopsis* within the
492 Lomentariaceae (Fig. 1), which was expected given that it has the diagnostic characteristics
493 of this family (tetrahedrally divided tetrasporangia, three-celled carpogonial branches and
494 characteristic lomentariaceous fusion cell in carposporophyte development, Lee et al. 1988,
495 Saunders et al. 1999, Le Gall et al. 2008). The only species, *B. caespitosa*, was closely
496 allied to *Lomentaria hakodatensis* (Fig. 1). While *Binghamiopsis* features thalli with a
497 multilayered cortex and loosely interwoven medullary filaments in a central cavity (Lee *et*.
498 *al.* 1988), *L. hakodatensis* is characterized by thalli with cortical and medullary layers
499 surrounding a central cavity that is articulated at various intervals by multi-rowed cellular
500 septa (Lee 1978). As *L. hakodatensis* was polyphyletic relative to *Lomentaria* sensu stricto,
501 its proper generic-level assignment awaits future assessments of *Lomentaria* (see below);
502 however, such substantial differences in thallus construction between *B. caespitosa* and *L.*
503 *hakodatensis* warrant their recognition as belonging to distinct genera.

504 The genericity of *Chamaeobotrys*, *C. boergesenii*, was resolved within the
505 Rhodymeniaceae (Fig. 1) where it was placed by Huisman (1996) when he established this
506 genus to accommodate some taxa originally assigned to another rhodymeniacean genus,
507 *Coelarthrum*. Based on the species included here, his decision to recognize *Chamaeobotrys*
508 was fully supported (Fig. 1). Unfortunately, our analyses did not include the genericity of
509 *Coelarthrum*, *C. cliftonii*, and therefore, the distinction of *Coelarthrum* and *Chamaeobotrys*
510 remains untested by molecular analyses.

511 At the time that Moe (1979) described the only crustose rhodymenialean taxon,
512 *Minium parvum*, only two families (Champiaceae and Rhodymeniaceae) were recognized
513 in the order. The criteria delimiting these families was greatly contested and poorly
514 understood and Moe (1979) struggled to assign the monospecific genus *Minium* to either
515 group especially after observing a variety of characteristics (tetrasporangial nemathecium,
516 auxiliary cell branches with their associated sterile cells and the arrangement of the cells in
517 the three-celled carpogonial branch) that did not ally *Minium* to either family. Moe (1979)
518 determined that the genus was best placed in the Rhodymeniaceae on account of a solid
519 thallus construction, cruciately divided tetrasporangia and the overall appearance and
520 development of the carposporophyte. Our molecular results solidly resolved *Minium* within
521 the Fryeellaceae as an unexpected close sister to *Fryella gardneri* (Fig. 1). Analysis of
522 tetrasporangial collections will confirm if one of the diagnostic features of the Fryeellaceae,
523 the adventitious growth of the cortex in the formation of tetrasporangia and short, 3-4
524 celled paraphyses, is also characteristic of *Minium*. Those observations will be included in a
525 future manuscript specific to rhodymenialean diversity in Canada.

526 527 *Assessment of select polyphyletic genera*

528 The present study was consistent with a previous molecular study that failed to resolve the
529 type of the genus *Erythrymenia*, *E. obovata* from South Africa, and *E. minuta* from
530 Australia as monophyletic (Saunders et al. 2006). To accommodate *E. minuta* we
531 established the novel monospecific genus *Perbella*, which was solidly resolved as sister to
532 *Hymenocladia* (Fig. 1). The latter two genera are distinguished primarily by tetrasporangial
533 division patterns, which are tetrahedral in *Hymenocladia* and cruciate in *Perbella*,

534 respectively. Additionally, *Perbella* is characterized by obovate blades while
535 *Hymenocladia* features pinnate blades (e.g. *H. usnea*) or complanate, broad, palmate,
536 subdichotomously divided blades (e.g. *H. chondricola*, Womersley 1996). Nonetheless, we
537 uncovered inconsistencies and taxonomic confusion in the literature related to the
538 identification of *E. minuta* (= *P. minuta*) relative to species of *Hymenocladia*. Specimens of
539 *H. conspersa* collected by Harvey from Garden Island, Western Australia (Trinity College
540 Dublin Herbarium, TCD) included foliose, irregularly divided plants with abundant laminar
541 and marginal tooth-like proliferations [Harvey 132, TCD, annotated “type” by Womersley,
542 lectotypified by Lewis (1994)] and separately mounted smaller obovate plants (Harvey
543 300-A, TCD). Harvey (1862) considered the former to be mature *H. conspersa* while the
544 latter were juveniles. Additional juvenile specimens were collected from Port Fairy,
545 Victoria (e.g. Harvey 300-D, TCD). Lewis (1994) and Womersley (1996) concluded that
546 Harvey’s “juveniles” were actually *E. minuta* (= *P. minuta*). Further, they speculated that
547 the juvenile *H. conspersa* specimens (that they attributed to *E. minuta*), reportedly from
548 Western Australia, were likely collected from Port Fairy, Victoria (Lewis 1994). Owing to
549 the previous, Lewis (1994) and Womersley (1996) interpreted *H. conspersa* as limited to
550 Western Australia with *E. minuta* (= *P. minuta*) restricted to Victoria.

551 As part of an ongoing barcode (COI-5P) survey of southern Australia (South
552 Australia, Victoria and Tasmania), three genetic species groups were resolved for
553 *Hymenocladia* including *H. chondricola*, *H. conspersa* and *H. usnea*. The first two were
554 closely related species groups (1.24% maximum interspecific variation in COI-5P) and are
555 in need of further molecular study. Our specimens identified as *H. chondricola* sensu stricto
556 (Fig. 6) were restricted to South Australia while collections attributed to *H. conspersa* were
557 more widely distributed from South Australia, Tasmania and Victoria and included mature
558 lanceolate morphs (Fig. 6b), intermediate morphs (Fig. 6c) and small, obovate juvenile
559 morphs (Fig. 6d) similar to those collected by Harvey and superficially reminiscent of *P.*
560 *minuta* specimens (Fig. 6e). As the type of *H. conspersa* is from Western Australia and our
561 isolates from southern Australia lacked the laminar papillae considered by Harvey (1862) to
562 be characteristic of this species (Fig. 6b), our assignment of *H. conspersa* remains tentative
563 pending inclusion of topotype material. If our collections do represent *H. conspersa*, we

564 provide genetic evidence that this species is indeed found in southern Australia and that
565 small plants resembling *P. minuta* should be considered with caution as they are potentially
566 juveniles of *H. conspersa*.

567 Previous and current phylogenetic assessments have consistently resolved the
568 speciose genus *Lomentaria* as polyphyletic (e.g., Le Gall et al. 2008). Our molecular
569 analyses resolved species assigned to *Lomentaria* as four independent lineages in the
570 Lomentariaceae (Fig. 1). The type of *Lomentaria*, *L. articulata*, was joined by *L. clavellosa*
571 and *L. orcadensis* (Fig. 1). As *L. articulata* features branches with multilayered septa and *L.*
572 *clavellosa* and *L. orcadensis*, have multilayered plugs only at the branch base, results herein
573 do not support previously recommended revisions of this genus based on thallus
574 construction and septation (Irvine & Guiry 1983). Thus, *Lomentaria* sensu stricto remains a
575 broadly defined genus characterized by various modes of thallus construction, tetrahedrally
576 divided tetrasporangia in invaginated sori and conical cystocarps with prominent pores (Lee
577 1978).

578 The novel genus *Fushitsunagia* was established to accommodate *L. catenata*, which
579 was resolved as sister to *Ceratodictyon* (Fig. 1). These genera are distinguished by
580 tetrasporangial division patterns, which are tetrahedral in *F. catenata* (Lee 1978) and
581 cruciate in *Ceratodictyon* (Price & Kraft 1991). The genus *Fushitsunagia* is unique from
582 other lomentariacean taxa in that during tetrasporangial development, medullary cells
583 become modified and form a conspicuous filamentous network that surrounds the
584 developing tetrasporangia (Lee 1978).

585 The remaining *Lomentaria* species included in our multigene analyses, *L. divaricata*
586 and *L. hakodatensis*, were resolved as sister to *Stirnia* and *Binghamiopsis*, respectively (Fig.
587 1). *Lomentaria divaricata* is distinguished from *Stirnia* according to thallus structure
588 (hollow in the former and solid in the later) and the respective production of spermatangia
589 and tetrasporangia on specialized fertile proliferations described only for the latter genus
590 (Wynne 2001). *Lomentaria hakodatensis* is separated from *Binghamiopsis* based on overall
591 thallus construction (see above). There are two available names to accommodate *L.*
592 *divaricata* and *L. hakodatensis*: *Hooperia* J. Agardh (1896), which would apply directly to
593 its generitype taxon *L. divaricata* and, *Chondrosiphon* Kützinger (1843) for which the

594 generitype species, *L. firma*, was not available for inclusion in our molecular analyses. As *L.*
595 *firma* shares numerous vegetative and reproductive characteristics with *L. hakodatensis*
596 (flattened thalli, anastomosed intricate branches and well-developed cortication formed of a
597 single layer of pigmented cells and 3-4 inner layers of subcortical cells, Curiel et al. 2006)
598 it seems likely that these taxa will resolve together in the resurrected genus *Chondrosiphon*;
599 however, it is possible that *L. firma* will resolve with *L. divaricata*, which would render
600 *Hooperia* a synonym of *Chondrosiphon* necessitating a new genus for *L. hakodatensis*.
601 Until *L. firma* is molecularly assessed, *L. divaricata* and *L. hakodatensis* should remain
602 *incertae sedis* in the Lomentariaceae. While we have established *Lomentaria* sensu stricto
603 as a monophyletic lineage and clarified some of its taxonomic conflicts, there remains
604 significant molecular and morphological work until this genus and the many species
605 attributed to it are properly assigned.

606 Recent molecular assessment of Australian species assigned to *Gloiosaccion* [*G.*
607 *brownii* Harvey (including *G. brownii* var. *firmum* and *G. brownii* var. *coriaceum*) and *G.*
608 *pumilum* J. Agardh], in relation to species of *Chrysomenia* [including the generitype species
609 *C. ventricosa* (J.V. Lamouroux) J. Agardh] warranted transfer of the former genus to the
610 latter (Schmidt et al. 2016). In that study, “*G.*” *brownii* var. *firmum* (collected from South
611 Australia) was supported as distinct from “*G.*” *brownii* var. *coriaceum* (collected from
612 Western Australia) and the latter variety was raised to specific rank (Schmidt et al. 2016).
613 Our routine barcoding studies in Australia have resolved collections (n= 31) field assigned
614 to “*G.*” *brownii* in five genetically distinct morphologically cryptic species groups (data
615 not shown). Two of those groups (one being our concept of “*G.*” *brownii*, which included
616 specimens collected from near the type locality, Tasmania) were included in the current
617 study (Fig. 1, Table S1). The *rbcL* data from our two “*G.*” *brownii* genetic groups did not
618 match the GenBank *rbcL* data representative of “*G.*” *brownii* or “*G.*” *coriacea* from the
619 Schmidt et al. (2016) study and further study of “*G.*” *brownii* from Australia is needed.

620 Consistent with Le Gall et al. (2008), our analyses resolved the genus *Chrysomenia*
621 as polyphyletic with one of the species, *C. wrightii* most closely related to *Botryocladia*
622 *leptopoda* (rendering this genus polyphyletic as well). Assessment of that conundrum was
623 beyond the scope of this study. Future molecular assessments including the generitype taxa

624 for *Botryocladia*, *Chrysomenia* and *Cryptarachne* (previously recognized as a subgenus or
625 a section of *Chrysomenia*, Guiry & Guiry 2015) are needed to clarify the species
626 appropriately assigned to those genera.

627 Former morphological and molecular assessments of rhodymenialean taxa also
628 identified the close alliance between *Cordylecladia erecta* and species of *Rhodymenia*,
629 which are distinguished primarily according to habit (Brodie & Guiry 1988, Millar et al.
630 1996, Saunders et al. 1999). The addition of *R. delicatula* here goes further by resolving as
631 sister to *C. erecta* and calling into question monophyly of *Rhodymenia* (Fig. 1). While *C.*
632 *erecta* features fully terete axes, species of *Rhodymenia* are typically compressed or foliose;
633 however, the recent description of the novel Australian species *R. compressa*, which
634 features compressed and sparsely branched thalli (Filloramo & Saunders *in press*),
635 challenges the utility of thallus habit for distinguishing *C. erecta* from *Rhodymenia* spp.
636 and more study is needed.

637

638 *Taxonomic reassessment of Drouetia*

639 Prior to this study inclusion of the monotypic genus, *Drouetia* in molecular analyses has
640 been uncertain due to frequent misidentifications of numerous taxa currently assigned to
641 *Asteromenia* and *Halichrysis* as the reportedly cosmopolitan generitype of *Drouetia*, *D.*
642 *coalescens* (Saunders et al. 2006). A recent study resolved material from South Africa that
643 was vegetatively representative of *Drouetia* and identified as “*D. coalescens*” as an
644 independent lineage in the Rhodymeniaceae (Saunders et al. 2006). In that study, Saunders
645 et al. (2006) viewed a prepared mica slide of holotype tetrasporangial material for the
646 generitype, *D. coalescens*, and reported what they interpreted as adventitious growth of the
647 cortex to form nemathecium of paraphyseal filaments and tetrasporangia on the dorsal surface
648 only. Those observations were inconsistent with reports of tetrasporangial development for
649 the South African samples (terminal tetrasporangia on both surfaces, Norris 1991) which,
650 as a result, were not regarded as representative of *D. coalescens* (Saunders et al. 2006). The
651 present study resolved three novel species from Australia as morphologically assignable to
652 the genus *Drouetia* (none were consistent with *D. coalescens*) and two of these were
653 included in multigene phylogenetic analyses where they were resolved in the

654 Rhodymeniaceae sister to the previously discussed South African collection (Fig. 1). Our
655 observation of tetrasporangial development for the novel species *D. viridescens* did not
656 suggest adventitious cortical growth in the formation of the tetrasporangial nemathecia (i.e.,
657 true paraphyses were absent) as reported by Saunders et al. (2006) for the generitype, which
658 prompted re-examination of holotype material of *D. coalescens* to clarify tetrasporangial
659 development for this genus. That material was provided on loan from the Farlow
660 Herbarium (FH) and freshly prepared sections were examined. We observed cruciately
661 divided tetrasporangia deeply embedded in the dorsal cortex only (Fig. 5, b and c).
662 Tetrasporangial initials developed from the cells of the inner cortex and during maturation,
663 became elongated and swollen, which resulted in neighbouring cortical cells becoming
664 compressed and elongated between the developing tetrasporangia, taking on the appearance
665 of paraphyses (Fig. 5, c-e). This mode of development was more consistent with that
666 observed in *D. viridescens* and other rhodymeniacean taxa, which are typically
667 characterized by tetrasporangia that differentiate from pre-existing cortical cells and lack
668 true adventitious filaments (paraphyses; Le Gall et al. 2008, Saunders & McDonald 2010).
669 More study of tetrasporangial development for the South African collections is needed to
670 determine if previous reports of tetrasporangial sori occurring on both sides of the blade
671 (Norris 1991) are incorrect and confounded by taxonomic misidentifications or if that
672 species has an atypical mode of development. Either way, the South African species
673 represents a fifth species best assigned to *Drouetia*, a conclusion that ultimately awaits
674 inclusion of *D. coalescens* in phylogenetic analyses to provide molecular confirmation, as
675 well as our decision to assign the three Australian species *D. aggregata*, *D. scutellata* and
676 *D. viridescens* to *Drouetia* as distinct from the generitype.

677

678

CONCLUSIONS

679 The intention of this study was to enhance understanding of evolutionary relationships in
680 the Rhodymeniales. Fast-site removal successfully improved resolution at a key node and
681 provided clarification of interfamilial relationships. By expanding taxonomic representation
682 we have addressed the phylogenetic affinities of rhodymenial genera absent from
683 previous molecular assessments and have clarified two consistently polyphyletic genera.

684 Additionally, re-examination of holotype material for *Drouetia coalescens* clarified
685 rhodymeniacean tetrasporangial development for the genus and provided evidence that the
686 three novel Australian species are correctly assigned to this genus, and that this genus is
687 correctly assigned to the Rhodymeniaceae.

688

689

ACKNOWLEDGEMENTS

690

691

692

693

694

695

696

697

698

699

700

701

702

703

704

705

REFERENCES

706

707

708

709

710

711

712

713

Agardh, J.G. 1896. Analecta algologica, Continuatio III. *Lunds Universitets Års-Skrift*,
Andra Afdelningen, Kongl. Fysiografiska Sällskapet i Lund Handlingar 32:1-140.

Bliding C. 1928. Studien über die Florideenordnung Rhodymeniales. *Universitets Årsskrift*
Ny Följd Lunds 24:1-74.

Brinkmann, H. & Philippe, H. 1999. Archaea sister group of Bacteria? Indications from tree
reconstruction artifacts in ancient phylogenies. *Mol. Biol. Evol.* 16:817-25.

714
715 Brodie, J. & Guiry, M. D. 1988. Life history of *Cordylecladia erecta*. *Brit. Phycol. J.*
716 23:347-64.
717
718 Cocquyt, E., Verbruggen, H., Leliaert, F. & De Clerck, O. 2010. Evolution and cytological
719 diversification of the green seaweeds (Ulvophyceae). *Mol. Biol. Evol.* 27:2052-61.
720
721 Curiel, D., Bellemo, G., Scattolin, M. & Marzocchi, M. 2006. First report of *Lomentaria*
722 *hakodatensis* (Lomentariaceae, Rhodophyta) from the lagoon of Venice (Adriatic Sea,
723 Mediterranean). *Acta. Adriat.* 47:65-72.
724
725 Delsuc, F., Brinkmann, H. & Philippe, H. 2005. Phylogenomics and the reconstruction of
726 the tree of life. *Nat. Rev. Genet.* 6:361-75.
727
728 Filloramo, G.V. & Saunders, G.W. *in press*. Molecular-assisted alpha taxonomy of the
729 genus *Rhodymenia* (Rhodymeniaceae, Rhodymeniales) from Australia reveals overlooked
730 species diversity. *Eur. J. Phycol.*
731
732 Freshwater, D. W., Fredericq, S., Butler, B. S., Hommersand, M. H. & Chase, M. W. 1994.
733 A gene phylogeny of the red algae (Rhodophyta) based on plastid *rbcL*. *Proc. Natl. Acad.*
734 *Sci. USA* 91:7281-5.
735
736 Guiry, M.D. & Guiry, G.M. 2015. *Algaebase*. World-wide electronic publication, National
737 University of Ireland, Galway. <http://www.algaebase.org>; searched on 15 August 2015.
738
739 Harvey, W.H. 1862. *Phycologia australica*: or, a history of Australian seaweeds;
740 comprising coloured figures and descriptions of the more characteristic marine algae of
741 New South Wales, Victoria, Tasmania, South Australia, and Western Australia, and a
742 synopsis of all known Australian algae. Vol. 4. pp. viii, Plates CLXXXI-CCXL. Lovell
743 Reeve & Co., London, 254 pp.

744

745 Ho, S. Y. W. & Jermiin, L. S. 2004. Tracing the decay of the historical signal in biological
746 sequence data. *Syst. Biol.* 53:623-37.

747

748 Holton, T. A. & Pisani, D. 2010. Deep genomic-scale analyses of the Metazoa reject
749 Coelomata: evidence from single- and multigene families analyzed under a supertree and
750 supermatrix paradigm. *Genome Biol. Evol.* 2:310-24.

751

752 Huisman, J. M. 1996. The red algal genus *Coelarthrum* Børgesen (Rhodymeniaceae,
753 Rhodymeniales) in Australian seas, including the description of *Chamaeobotrys* gen. nov.
754 *Phycologia* 35:95-112.

755

756 Irvine, L. M. & Guiry, M. D. 1983. Rhodymeniales. In Irvine, L.M. [Ed.] *Seaweeds of the*
757 *British Isles. Vol. 1. Rhodophyta. Part 2A. Cryptonemiales (sensu stricto), Palmariales,*
758 *Rhodymeniales.* British Museum (Natural History), London, pp. 73-98.

759

760 Jeffroy, O., Brinkmann, H., Delsuc, F. & Philippe, H. 2006. Phylogenomics: the beginning
761 of incongruence? *Trends Genet.* 22:225-31.

762

763 Kearse, M., Moir, R., Wilson, A., Stones-Havas, S., Cheung, M., Sturrock, S., Buxton, S.,
764 Cooper, A., Markowitz, S., Duran, C., Thierer, T., Ashton, B., Mentjies, P. & Drummond,
765 A. 2012. Geneious Basic: an integrated and extendable desktop software platform for the
766 organization and analysis of sequence data. *Bioinformatics* 28:1647-9.

767

768 Kostka, M., Uzlikova, M., Cepicka, I. & Flegr, J. 2008. SlowFaster, a user-friendly
769 program for slow-fast analysis and its application on phylogeny of *Blastocystis*. *BMC*
770 *Bioinformatics* 9:341-6.

771

772 Kützing, F.T. 1843. *Phycologia generalis* oder anatomie, physiologie und systemkunde der
773 tange. Mit 80 farbig gedruckten tafeln, gezeichnet und gravirt vom verfasser. pp. [part 1]:
774 [i]-xxxii, [1]-142, [part 2:] 143-458, 1, err.], pls 1-80. Leipzig: F.A. Brockhaus.
775
776 Kylin, H. 1931. Die Florideenordnung Rhodymeniales. *Acta. Univ. Lundensis* 27:1-48.
777
778 Lanfear, R., Calcott, B., Ho, S. Y. W. & Guindon, S. 2012. PartitionFinder: combined
779 selection of partitioning schemes and substitution models for phylogenetic analyses. *Mol.*
780 *Biol. Evol.* 29:1695-1701.
781
782 Le Gall, L. L., Dalen, J. L. & Saunders, G. W. 2008. Phylogenetic analyses of the red algal
783 order Rhodymeniales supports recognition of the Hymenocladaceae fam. nov.,
784 Fryellaceae fam. nov., and *Neogastroclonium* gen. nov. *J. Phycol.* 44:1556-71.
785
786 Le Gall, L. L. & Saunders, G. W. 2007. A nuclear phylogeny of the Florideophyceae
787 (Rhodophyta) inferred from combined EF2, small subunit and large subunit ribosomal
788 DNA: establishing the red algal subclass Corallinophycidae. *Mol. Phylogenet. Evol.*
789 43:1118-30.
790
791 Lee, I. K. 1978. Studies on Rhodymeniales from Hokkaido. *J. Fac. Sci. Hokkaido Univ. Ser.*
792 *V (Bot.)* 11:1-203.
793
794 Lee, I. K., West, J. A. & Hommersand, M. H. 1988. *Binghamiopsis caespitose* gen. et sp.
795 nov. (Lomentariaceae, Rhodophyceae) from the eastern Pacific. *Korean J. Phycol.* 3:1-13.
796
797 Lewis, J. A. 1994. Transfer of the Australian red algae *Kallymenia nitophylloides* to
798 *Cryptonemia* (Halymeniaceae) and *Halymenia chondricola* to *Hymenocladia*
799 (Rhodymeniaceae). *Taxon* 43:3-10.
800

801 Millar, A. J. K., Saunders, G. W., Strachan, I. M. & Kraft, G. T. 1996. The morphology,
802 reproduction and small-subunit rRNA gene sequence of *Cephalocystis* (Rhodymeniaceae,
803 Rhodophyta), a new genus based on *Cordylecladia furcellata* J. Agardh from Australia.
804 *Phycologia* 35:48-60.

805

806 Moe, R. L. 1979. *Minium parvum* gen. et sp. nov., a crustose member of the
807 Rhodymeniales (Rhodophyta). *Phycologia* 18:38-46.

808

809 Morgan-Richards, M., Trewick, S. A., Bartosch-Haerlid, A., Kardailsky, O., Phillips, M. J.,
810 McLenachan, P. A. & Penny, D. 2008. Bird evolution: testing the Metaves clade with six
811 new mitochondrial genomes. *BMC Evol. Biol.* 8:20.

812

813 Norris, R. E. 1991. Some unusual marine red algae (Rhodophyta) from South Africa.
814 *Phycologia* 30:582-596.

815

816 Oltmanns, F. 1904. *Morphologie und Biologie der Algen*. Verlag von Gustav Fisher, Jena,
817 733 pp.

818

819 Pick, K. S., Phillipe, H., Schreiber, F., Erpenbeck, D., Jackson, D. J., Wrende, P., Wiens,
820 M., Alie, A., Morgenstern B., Manuel, M. & Wörheide, G. 2010. Improved phylogenomic
821 taxon sampling noticeably affects nonbilaterian relationships. *Mol. Biol. Evol.* 27:1983-7.

822

823 Pisani, D., Feuda, R., Peterson, K. J. & Smith, A. B. 2012. Resolving phylogenetic signal
824 from noise when divergence is rapid: a new look at the old problem of echinoderm class
825 relationships. *Mol. Phylogenet. Evol.* 62:27-34.

826

827 Price, I. R. & Kraft, G. T. 1991. Reproductive development and classification of the red
828 algal genus *Ceratodictyon* (Rhodymeniales, Rhodophyta). *Phycologia* 30:106-16.

829

830 Pond, S. L. K., Frost, S. D. W. & Muse, S. V. 2005. HyPhy: hypothesis testing using
831 phylogenies. *Bioinformatics* 21:676–9.

832

833 Ragan, M. A., Bird, C. J., Rice, E. L., Gutell, R. R., Murpy, C.A. & Singh, R. K. 1994. A
834 molecular phylogeny of the marine red algae (Rhodophyta) based on the nuclear small-
835 subunit rRNA gene. *Proc. Natl. Acad. Sci. USA* 91:7276-80.

836

837 Rodriguez-Ezpeleta, N., Brinkmann, H., Roure, B., Lartillot, N., Lang, B. F. & Phillipe, H.
838 2007. Detecting and overcoming systematic errors in genome-scale phylogenies. *Syst. Biol.*
839 56:389-99.

840

841 Ronquist, F. & Huelsenbeck, J. P. 2003. MrBayes 3: Bayesian phylogenetic tree selection.
842 *Syst. Biol.* 51:492-508.

843

844 Ruiz-Trillo, I., Riutort, M., Littlewood, D. T. J., Herniou, E. A. & Baguna, J. 1999. Acoel
845 flatworms: earliest extant bilaterian metazoans, not members of Platyhelminthes. *Science*
846 283:1919-23.

847

848 Saunders, G. W. & Hommersand, M. H. 2004. Assessing red algal supraordinal diversity
849 and taxonomy in the context of contemporary systematic data. *Am. J. Bot.* 91:1494-507.

850

851 Saunders, G. W. & Kraft, G. T. 1994. Small subunit rRNA gene sequences from
852 representatives of selected families of the Gigartinales and Rhodymeniales (Rhodophyta). 1.
853 Evidence for the Plocamiales ord. nov. *Can. J. Bot.* 72:1250-63.

854

855 Saunders, G. W. & Kraft, G. T. 1996. Small subunit rRNA gene sequences from
856 representatives of selected families of the Gigartinales and Rhodymeniales (Rhodophyta). 2.
857 Recognition of the Halymeniales ord. nov. *Can. J. Bot.* 74:694-707

858

859 Saunders, G. W. & McDevit, D. C. 2012. Methods for DNA barcoding photosynthetic
860 protists emphasizing the macroalgae and diatoms. *Methods Mol. Biol.* 858:207-22.
861

862 Saunders, G. W. & McDonald, B. 2010. DNA barcoding reveals multiple overlooked
863 Australian species of the red algal order Rhodymeniales (Florideophyceae), with
864 resurrection of *Halopeltis* J. Agardh and description of *Pseudohalopeltis* gen. nov. *Botany*
865 88:639-67.
866

867 Saunders, G. W. & Moore, T. E. 2013. Refinements for the amplification and sequencing of
868 red algal DNA barcode and RedToL phylogenetic markers: a summary of current primers,
869 profiles and strategies. *Algae* 28:31-43.
870

871 Saunders, G. W., Lane, C. E., Schneider, C. W. & Kraft, G. T. 2006. Unravelling the
872 *Asteromenia peltata* species complex with clarification of the genera *Halichrysis* and
873 *Drouetia* (Rhodymeniaceae, Rhodophyta). *Can. J. Bot.* 84:1581-607.
874

875 Saunders, G. W., Strachan, I. M. & Kraft, G. T. 1999. The families of the order
876 Rhodymeniales (Rhodophyta): a molecular-systematic investigation with a description of
877 Faucheaceae fam. nov. *Phycologia* 38:23-40.
878

879 Schmidt, W.E., Gurgel, C.F.D. & Fredericq, S. 2016. Taxonomic transfer of the red algal
880 genus *Gloiosaccion* to *Chrysymenia* (Rhodymeniaceae, Rhodymeniales), including the
881 description of a new species, *Chrysymenia pseudoventricosa*, for the Gulf of
882 Mexico. *Phytotaxa* 243: 54-70.
883

884 Schmitz, F. 1889. Systematische ubersicht der bisher bekannten gattungen der Florideen.
885 *Flora* 72:435-56.
886

887 Sjöstedt, L. G. 1926. Floridean studies. *Acta. Univ. Lundensis.* 22:1-95.
888

889 Stamatakis, A., Hoover, P. & Rougemont, J. 2008. A rapid bootstrapping algorithm for the
890 RAxML web-servers. *Syst. Biol.* 57:758-71.
891
892 Sparling, S. R. 1957. The structure and the reproduction of some members of the
893 Rhodymeniaceae. *Univ. Calif. Publ. Bot.* 29:319-96.
894
895 Sperling, E. A., Peterson, K. J. & Pisani, D. 2009. Phylogenetic-signal dissection of nuclear
896 housekeeping genes supports the paraphyly of sponges and the monophyly of Eumetazoa.
897 *Mol. Biol. Evol.* 26:2261-74.
898
899 Taylor, W.R. 1945. Pacific marine algae of the Allan Hancock Expeditions to the
900 Galapagos Islands. *Allan Hancock Pac. Exped.* 12:1-528.
901
902 Verbruggen, H. 2012. SiteStripper v.1.01. GNU General Public
903 License. <http://www.phycoweb.net/software/SiteStripper/index.html>
904
905 Verbruggen, H., Ashworth, M., LoDuca, S. T., Vlaeminck, C., Cocquyt, E., Sauvage, T.,
906 Zechman, F. W., Littler, D. S., Littler, M. M., Leliaert, F. & De Clerck, O. 2009. A multi-
907 locus time-calibrated phylogeny of the siphonous green algae. *Mol. Phylogenet.*
908 *Evol.* 50:642-53.
909
910 Verbruggen, H., Maggs, C. A., Saunders, G. W., Le Gall, L., Yoon, H. S. & De Clerck, O.
911 2010. Data mining approach identifies research priorities and data requirements for
912 resolving the red algal tree of life. *BMC Evol. Biol.* 10:16.
913
914 Waddell, P. J., Cao, Y., Hauf, J. & Hasegawa, M. 1999. Using novel phylogenetic methods
915 to evaluate mammalian mtDNA, including amino acid-invariant sites-LogDet plus site
916 stripping to detect internal conflicts in the data, with special reference to the positions of
917 hedgehog, armadillo, and elephant. *Syst. Biol.* 48:31-53.
918

- 919 Withall, R. & Saunders, G. W. 2006. Combining small and large subunit ribosomal DNA
920 genes to resolve relationships among orders of Rhodymeniophycidae (Rhodophyta):
921 recognition of the Acrosymphytales ord. nov. *Eur. J. Phycol.* 41:379-94.
922
- 923 Womersley, H. B. S. 1996. *The marine benthic flora of southern Australia – Part IIIB-*
924 *Gracilariales, Rhodymeniales, Corallinales and Bonnemaisoniales*. Vol. 5. Australian
925 Biological Resources Study & the State Herbarium of South Australia, Canberra &
926 Adelaide, 392 pp.
927
- 928 Wynne, M. J. 2001. *Stirnia prolifera* gen. et sp. nov. (Rhodymeniales, Rhodophyta) from
929 the Sultanate of Oman. *Bot. Mar.* 44:163-9.
930
- 931 Zeng, L., Zhang, Q., Sun, R., Kong, H., Zhang, N. & Ma, H. 2014. Resolution of deep
932 angiosperm phylogeny using conserved nuclear genes and estimates of early divergence
933 times. *Nat. Commun.* 5:1-12.
934

935 FIGURE LEGENDS

936 **Figure 1.** RAxML phylogeny for full multigene alignment partitioned by gene and then
937 codon with subfamilial bootstrap support values appended. Branch letters correspond to the
938 support values in Table 2. Taxa in bold represent generitype species. Asterisks denote fully
939 supported branches. Species transferred to new genera have the previous genus name in
940 brackets. Outgroup species of the Halymeniales and Sebdeniales were compressed to
941 ordinal level to facilitate presentation.

942

943 **Figure 2.** *Drouetia aggregata* Filloramo & G.W. Saunders sp. nov.

944 a. Top view of vegetative holotype (GWS032793). Scale bar = 8.75 mm.

945 b. Side view of vegetative holotype with distinct stipes subtending anastomosed blades
946 (GWS032793). Scale bar = 8 mm.

947 c. Transverse section at mid-thallus showing medulla and dorsiventral aspect
948 (GWS032793). Scale bar = 200 μ m.

949 d. Transverse section at mid-thallus showing ventral surface and aggregates of small cells
950 interspersed among the larger cells of the medulla (GWS032792). Scale bar = 100 μm .

951

952 **Figure 3.** *Drouetia scutellata* Filloramo & G.W. Saunders sp. nov.

953 a. Habit of single peltate blades showing distinct stipes and central depressions, lighter
954 patches indicate spermatangial sori (arrows) (Isotype, GWS032752). Scale bar = 1 cm.

955 b. Habit of cystocarpic holotype (GWS032729). Scale bar = 1 cm.

956 c. Transverse section at mid-thallus showing medulla and dorsiventral aspect
957 (GWS032729). Scale bar = 100 μm .

958 d. Transverse section through mature cystocarp (GWS032729). Scale bar = 250 μm .

959 e. Transverse section of male plant showing spermatangial development on the dorsal
960 surface (GWS032752). Scale bar = 10 μm .

961

962 **Figure 4.** *Drouetia viridescens* Filloramo & G.W. Saunders sp. nov.

963 a. Habit of single peltate blades attached to substratum by single stipe (not pictured)
964 (GWS032740). Scale bar = 1 cm.

965 b. Habit of tetrasporic holotype showing anastomosed blades that form an irregular outline
966 (GWS032612). Scale bar = 1 cm.

967 c. Transverse section at mid-thallus of vegetative plant (GWS032682). Scale bar = 93 μm .

968 d. Transverse section at mid-thallus of tetrasporic holotype (GWS032612). Scale bar = 108
969 μm .

970 e. Mature cruciately divided tetrasporangium (GWS032612). Scale bar = 33 μm .

971 f. Transverse section at mid-thallus of tetrasporic holotype showing cortical cell (arrow)
972 compressed between developing and mature tetrasporangia creating the appearance of
973 paraphyses. Tetrasporangial initials pit connected (arrowheads) to inner cortical cell
974 (GWS032612). Scale bar = 25 μm .

975 g. Intercalary tetrasporangial initial pit connected (arrowheads) to two neighboring cortical
976 cells (GWS032612). Scale bar = 20 μm .

977

978 **Figure 5.** Tetrasporangial holotype of *Drouetia coalescens* (Farlow) G. De Toni (Harvard
979 University Herbaria & Libraries, No. 00777108).

980 a. Herbarium label and gross morphology of holotype. Scale bar = 21 mm.

981 b. Transverse section of tetrasporangial thallus showing dorsal tetrasporangial sorus. Scale
982 bar = 91 μm .

983 c. Developing tetrasporangia deeply embedded in the dorsal cortex. Scale bar = 47 μm .

984 d. Cruciate divided tetrasporangia (arrows). Scale bar = 23 μm .

985 e. Pit connection (arrow) between two cortical cells modified into tetrasporangia
986 surrounded by compressed cortical cells creating the appearance of paraphyses. Scale bar =
987 18 μm .

988

989 **Figure 6.** *Hymenocladia chondricola* (Sonder) J. Lewis, *Hymenocladia conspersa* (Harvey)

990 J. Agardh and *Perbella minuta* (Kylin) Filloramo & G.W. Saunders comb. nov.

991 a. Gross morphology of a vegetative specimen of *H. chondricola* from South Australia
992 (GWS029560). Scale bar = 25 mm.

993 b. Mature morphology of a vegetative specimen of *H. conspersa* from Victoria
994 (GWS017300). Scale bar = 25 mm.

995 c. Intermediate morphology of vegetative specimen of *H. conspersa* from Tasmania
996 (GWS015238). Scale bar = 19 mm.

997 d. Juvenile morphology of vegetative specimen of *H. conspersa* from Tasmania
998 (GWS016539). Scale bar = 13 mm.

999 e. Gross morphology of a vegetative specimen of *Perbella minuta* from Tasmania
1000 (GWS015206). Scale bar = 25 mm.

1001

1002 **Table 1.** Collection details and COI-5P GenBank accession numbers for Australian
1003 *Drouetia* samples used in molecular and morphological analyses. All samples were
1004 collected from Coffs Harbour, New South Wales, Australia. All data was generated for the
1005 present study.

1006

1007 **Table 2.** Bayesian posterior probabilities, RAxML bootstrap values and likelihood scores
1008 for the full multigene alignment with partitioning by gene and then codon (noPF) and with
1009 partitioning as determined by PartitionFinder (PF). RAxML bootstrap values and likelihood
1010 scores for the site-stripper subalignments with partitioning by gene and then codon (noPF).
1011 Dashes (-) indicate branch support below 50% and n/a indicates a branch that was not
1012 resolved.

1013

1014 **Table 3.** Intraspecific COI-5P divergence and distance to nearest neighbour for Australian
1015 species of *Drouetia* included in this study.

1016 SUPPLEMENTARY MATERIAL

1017

1018 **Figure. S1.** An alternative topology produced by neighbor-joining analysis with the HKY
1019 model to assess the impact of the starting tree on SiteStripper analyses.

1020

1021 **Table S1.** List of species and voucher numbers used in this study. GenBank sequences in
1022 bold were generated for this study. Generitype species are noted with an asterisk. ND
1023 indicates data not generated for this study. Percent (%) complete is based on the number of
1024 included sites out of the 8714 bp alignment. Collection details for all specimens are
1025 available on the BOLD website in the public dataset DS-RHDYPHY.

Table 1. Collection details and COI-5P GenBank accession numbers for Australian *Drouetia* samples used in molecular and morphological analyses. All samples were collected from Coffs Harbour, New South Wales, Australia. All data was generated for the present study

Species	Voucher			COI-5P GenBank
	Number	Habitat	Geography	Accession
<i>Drouetia aggregata</i> Filloramo & G.W. Saunders	GWS032792	4 m on rock	Mutton Bird Island (South)	KU707859
	GWS032793	4 m on rock	Mutton Bird Island (South)	KU707873
<i>Drouetia scutellata</i> Filloramo & G.W. Saunders	GWS032664	6 m on invert	South Solitary Island (Southeast)	KU707850
	GWS032729	5 m on rock	Mutton Bird Island (North)	KU707846
	GWS032752	5 m on invert	Mutton Bird Island (North)	KU707880
<i>Drouetia viridescens</i> Filloramo & G.W. Saunders	GWS032599	5 m on rock	Korora Beach	KU707869
	GWS032600	5 m on rock	Korora Beach	KU707868
	GWS032612	8 m on rock	Split Solitary Island (Northwest)	KU707855
	GWS032624	8 m on rock	Split Solitary Island (Northwest)	KU707881
	GWS032642	10 m on invert	Split Solitary Island (East)	KU707878
	GWS032643	10 m on coral rubble	South Solitary Island (East)	KU707874
	GWS032665	6 m on invert	South Solitary Island (Southeast)	KU707863
	GWS032672	10 m on invert	Black Rock	KU707870

Table 1. Collection details and COI-5P GenBank accession numbers for Australian *Drouetia* samples used in molecular and morphological analyses. All samples were collected from Coffs Harbour, New South Wales, Australia. All data was generated for the present study

Species	Voucher			COI-5P GenBank
	Number	Habitat	Geography	Accession
	GWS032682	6 m on invert	Black Rock	KU707847
	GWS032740	5 m on invert	Mutton Bird Island (North)	KU707852

Author Manuscript

Table 2. Bayesian posterior probabilities, RAxML bootstrap values and likelihood scores for the full multigene alignment with partitioning by gene and then codon (noPF) and with partitioning as determined by PartitionFinder (PF). RAxML bootstrap values and likelihood scores for the site-stripper subalignments with partitioning by gene and then codon (noPF). Dashes (-) indicate branch support below 50% and n/a indicates a branch that was not resolved.

	Bayes		RAxML		RAxML					
	100%				95%	90%	85%	80%	75%	70%
	noPF	PF	noPF	PF	noPF					
% of sites retained	-143267	-143395	-143595	-143787	-112089	-86686	-65296	-47116	-32139	-20852
A	1	1	100	100	100	100	100	100	100	100
B	1	1	95	95	93	95	97	99	98	79
C	n/a	-	-	50	n/a	51	68	75	65	62
D	1	1	100	100	100	100	100	100	100	100
E	1	1	100	100	100	100	100	100	100	100
F	1	1	100	100	100	100	100	100	100	100
G	1	1	100	100	100	100	100	100	100	98
H	1	1	100	100	100	100	100	100	100	100
I	1	1	79	80	71	78	71	81	71	80
J	1	1	100	100	100	100	100	100	100	100

Table 3. Intraspecific COI-5P divergence and distance to nearest neighbour for Australian species of *Drouetia* included in this study.

Species	Max intraspecific divergence (%)	Nearest species	Distance to nearest neighbour (%)
D. aggregata (n= 2)	0	D. scutellata	7.19
D. scutellata (n= 3)	0.15	D. viridescens	2.5
D. viridescens (n= 11)	0.31	D. scutellata	2.5

Author Manuscript

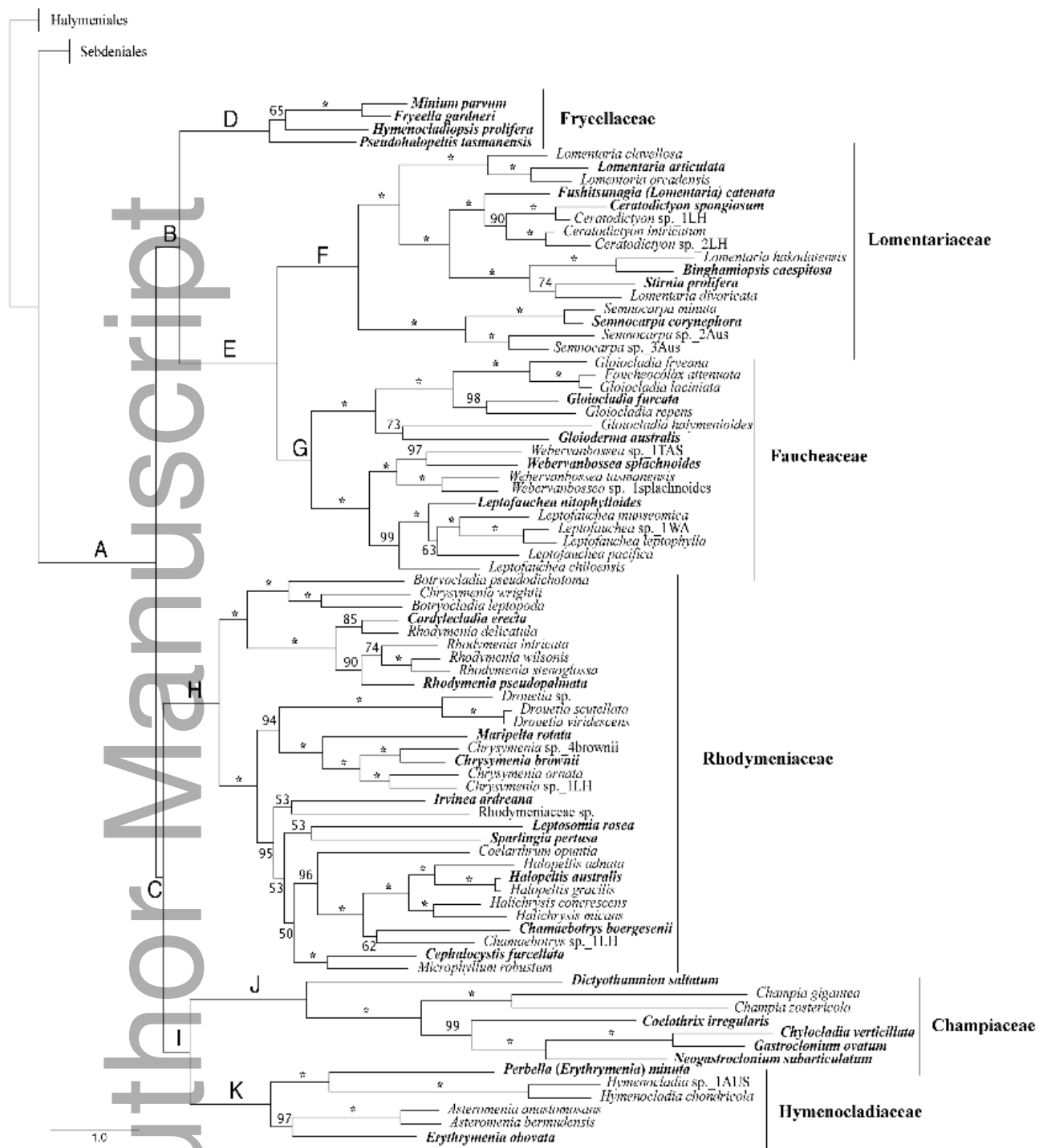
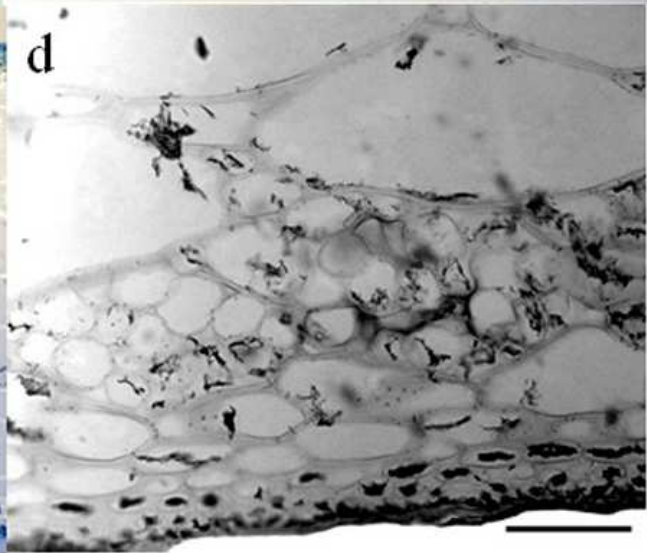
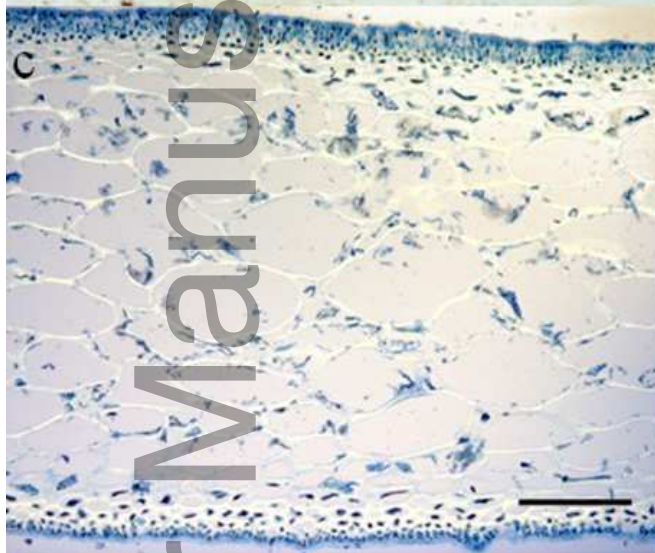
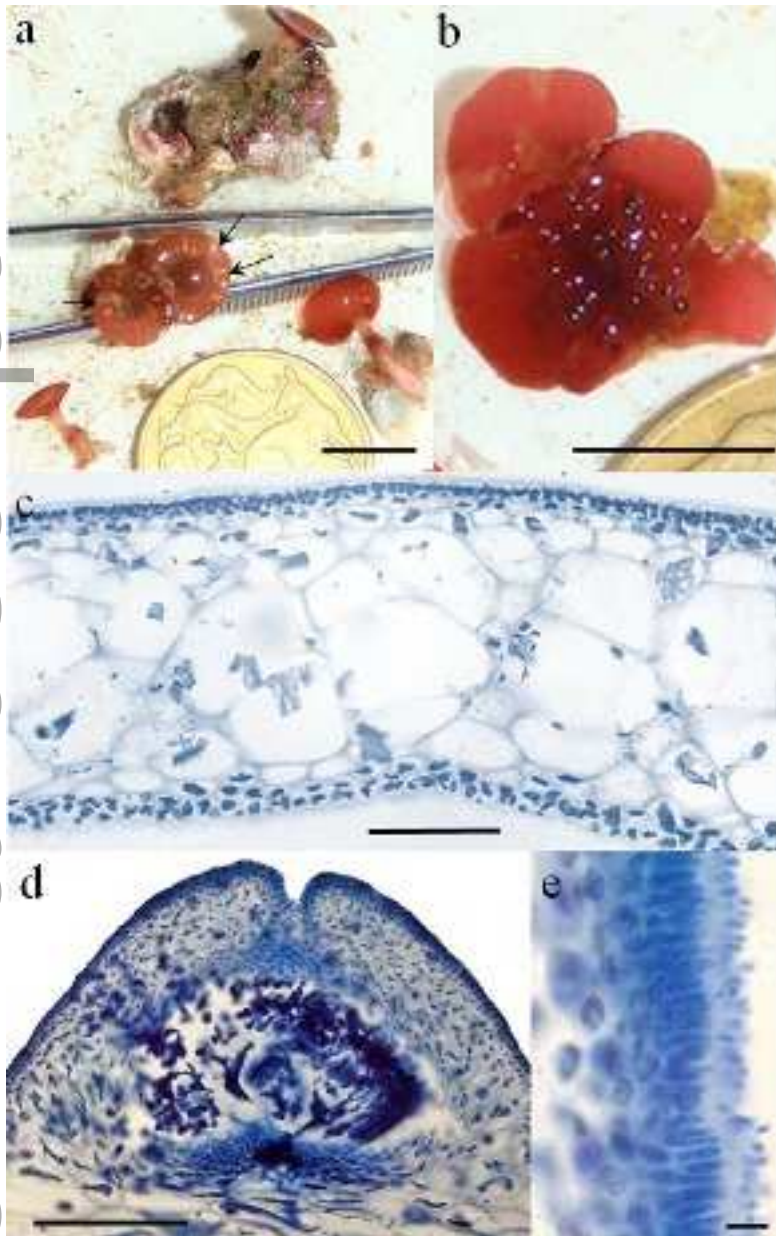


Figure 1.

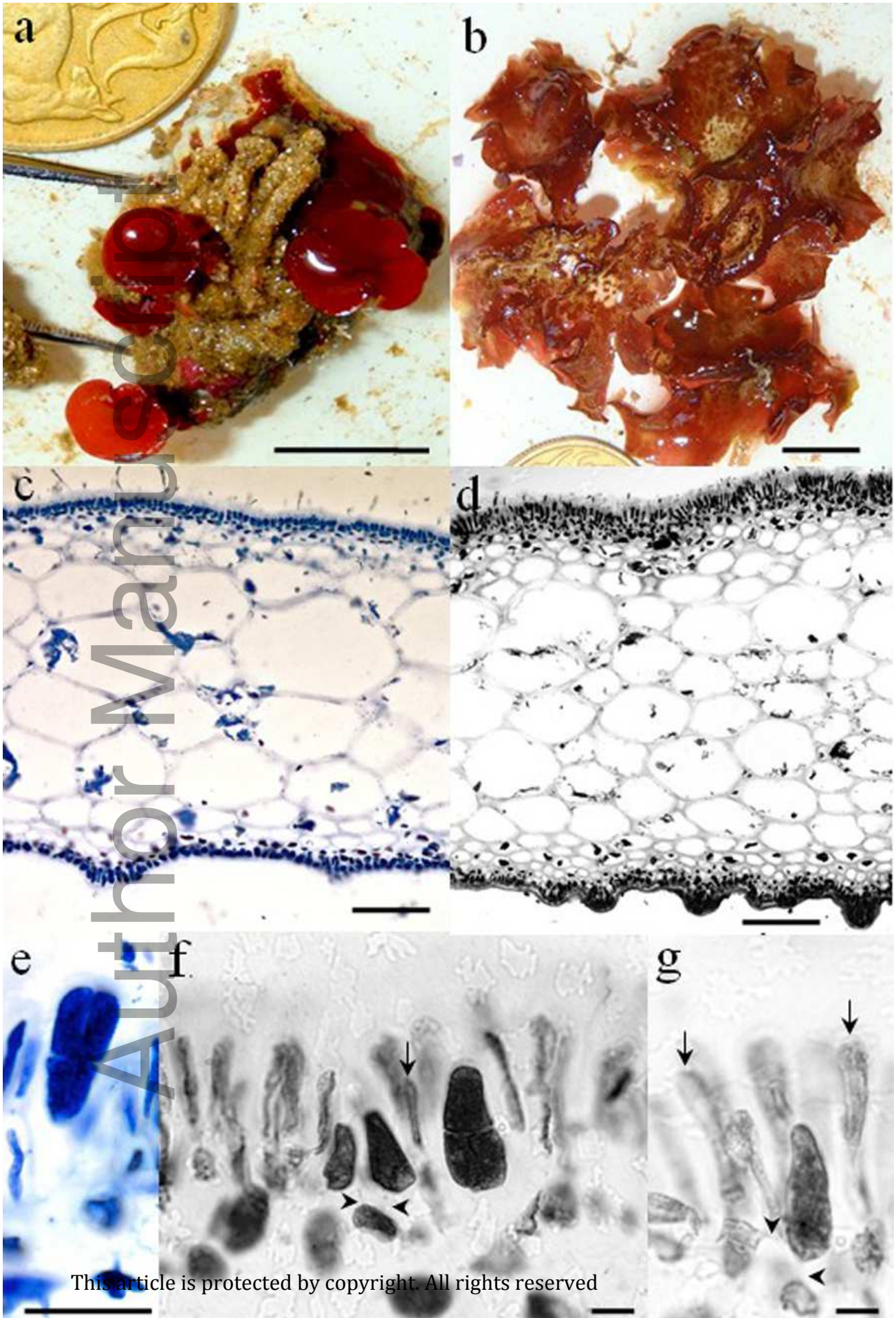
jpy_12418-15-207_f1.tif



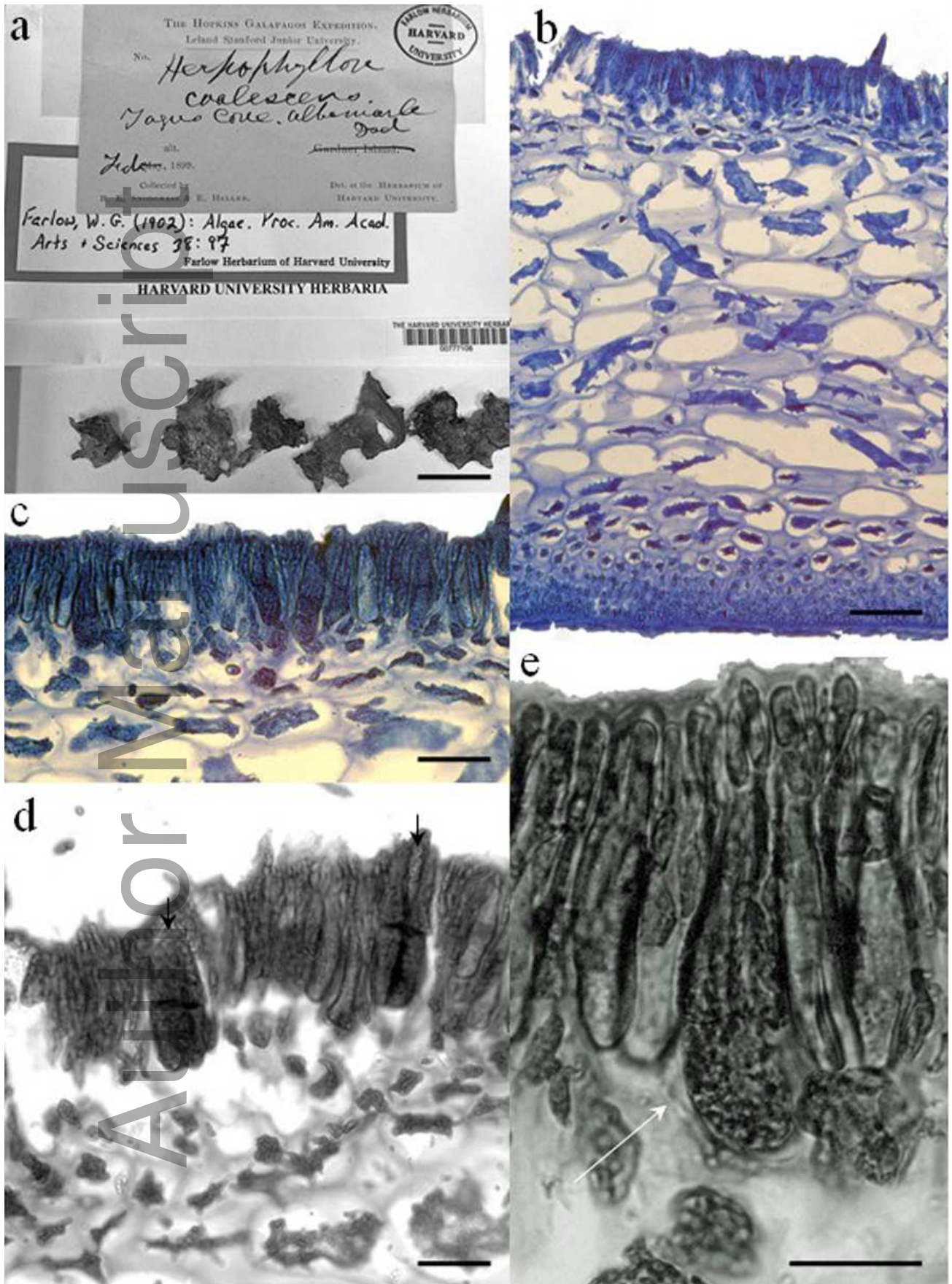
jpy_12418-15-207_f2.tif



jpy_12418-15-207_f3.tif



This article is protected by copyright. All rights reserved



jpy_12418-15-207_f5.tif



Figures 23-27

jpy_12418-15-207_f6.tif